



# CHORUS

This is the accepted manuscript made available via CHORUS. The article has been published as:

## G-type antiferromagnetic order in the metallic oxide

### $\text{LaCu}_{\{3\}}\text{Cr}_{\{4\}}\text{O}_{\{12\}}$

Takashi Saito (□□□□), Shoubao Zhang (□□□), Dmitry Khalyavin, Pascal Manuel, J. Paul Attfield, and Yuichi Shimakawa (□□□□)

Phys. Rev. B **95**, 041109 — Published 20 January 2017

DOI: [10.1103/PhysRevB.95.041109](https://doi.org/10.1103/PhysRevB.95.041109)

## G-type antiferromagnetic order in the metallic oxide $\text{LaCu}_3\text{Cr}_4\text{O}_{12}$

Takashi Saito (齊藤高志),<sup>1,\*</sup> Shoubao Zhang (张守宝),<sup>1</sup> Dmitry Khalyavin,<sup>2</sup> Pascal Manuel,<sup>2</sup> J. Paul Attfield,<sup>3</sup> and Yuichi Shimakawa (島川祐一)<sup>1,4</sup>

<sup>1</sup>Institute for Chemical Research, Kyoto University, Uji, Kyoto 611-0011, Japan

<sup>2</sup>ISIS, Rutherford Appleton Laboratory, Harwell Oxford, Didcot OX11 0QX, United Kingdom

<sup>3</sup>Centre for Science at Extreme Conditions and School of Chemistry, University of Edinburgh, Mayfield Road, Edinburgh EH9 3JZ, United Kingdom

<sup>4</sup>Japan Science and Technology Agency, CREST, Uji, Kyoto 611-0011, Japan

The *A*-site-ordered cubic perovskite  $\text{LaCu}_3\text{Cr}_4\text{O}_{12}$ , where a partial Cu-Cr inter-site charge transfer transition occurs at  $T_{\text{CT}} = 220$  K, was found to be an unconventional metallic and G-type antiferromagnetic oxide. Neutron powder diffraction revealed a G-type antiferromagnetic ordering at the Cr sites and no ordered moments at the Cu sites. *Ab initio* electronic structure calculations revealed that the narrowing of the Cr–O–Cr bands due to heavy tilting of the  $\text{CrO}_6$  octahedra and the strong hybridization of the Cu-3*d*, Cr-3*d* and O-2*p* orbitals near the Fermi level give an unusual electronic structure in the vicinity of a localized-electron regime. The G-type magnetic structure is primarily stabilized by nearest-neighbor antiferromagnetic superexchange interactions of the near-localized Cr spins. The ferromagnetic {1 1 1} layers of the G-type antiferromagnetic Cr-spin sublattice allow the spin-polarized electron transfer through the strongly hybridized Cu orbitals.

Transition-metal oxides show a wide variety of transport and magnetic properties because of the presence of the partially filled *d* orbitals of the transition-metal ions and the rather strong *pd* hybridization between oxygen 2*p* and metal *d* orbitals. The insulating oxides tend to be superexchange-driven antiferromagnets, where the metal *d* electrons are localized and give local magnetic moments, whereas many of the conducting oxides show Pauli paramagnetism without local moments. Oxides having spin-polarized conduction electrons are rare, and itinerant ferromagnets like  $\text{SrRuO}_3$  are of interest for their band ferromagnetism [1]. Double-exchange driven ferromagnets, where the localized *d* electrons are polarized ferromagnetically by Hund's coupling with the itinerant *d* electrons, as reported in  $\text{La}_{1-x}\text{Sr}_x\text{MnO}_3$  [2] and  $\text{CrO}_2$  [3] and ferrimagnetic double perovskites such as  $\text{Sr}_2\text{FeMoO}_6$  [4] also have spin-polarized conduction electrons.

Antiferromagnetism is generally incompatible with metallicity in oxides due to strong scattering of conduction electrons by antiparallel ordered spins. Very few conducting antiferromagnetic (AFM) oxides are reported and these all have ferromagnetic (FM) coupling between some nearest neighbor (NN) spins facilitating anisotropic conductivity. For example, the layered materials  $(\text{La,Sr})_3\text{Mn}_2\text{O}_7$  [5] and  $\text{Ca}_3\text{Ru}_2\text{O}_7$  [6] show metallic conductivity and have AFM stacking of FM bilayers where NN couplings are ferromagnetic. Perovskites  $\text{CaCrO}_3$  and  $\text{SrCrO}_3$  also have metallic conductivity and undergo AFM orderings of  $\text{Cr}^{4+}$  moments [7,8]. Although there have been conflicting reports on the transport behaviors of those compounds [9–15], recent optical conductivity [7,8] and photoemission spectroscopy [16] studies have revealed that their intrinsic transport is metallic. The AFM ordering in  $\text{CaCrO}_3$  and  $\text{SrCrO}_3$  stems from orbital ordering of the Cr *t*<sub>2g</sub> electrons associated with the distortion of the  $\text{CrO}_6$  octahedra [7–9, 17]. This results in C-type antiferromagnetism with AFM orbitally-ordered planes and FM NN couplings between the planes [7–9]. In this paper, we show that the cubic *A*-site-ordered perovskite  $\text{LaCu}_3\text{Cr}_4\text{O}_{12}$

has an unprecedented metallic G-type antiferromagnetic ground state where all NN spin-spin couplings are antiferromagnetic.

LaCu<sub>3</sub>Cr<sub>4</sub>O<sub>12</sub> crystallizes in the AA'<sub>3</sub>B<sub>4</sub>O<sub>12</sub>-type A-site-ordered perovskite structure shown in Fig. 1(a), where the CrO<sub>6</sub> octahedra are heavily tilted and Cu occupies 3/4 of the originally 12-fold coordinated A sites of the ABO<sub>3</sub> simple perovskite structure with a square-planar coordination (A' sites) [18,19]. At 220 K (= T<sub>CT</sub>) the compound undergoes an intersite charge transfer (CT) transition described as LaCu<sup>(2+δ)+</sup><sub>3</sub>Cr<sup>(3.75-0.75δ)+</sup><sub>4</sub>O<sub>12</sub> (T > T<sub>CT</sub>) ↔ LaCu<sup>(3-γ)+</sup><sub>3</sub>Cr<sup>(3+0.75γ)+</sup><sub>4</sub>O<sub>12</sub> (T < T<sub>CT</sub>). Both A'-site Cu and B-site Cr ions have mixed valence states at both above and below T<sub>CT</sub>, keeping the conductivity metallic down to 5 K with only a small anomaly at T<sub>CT</sub> [19]. This is in contrast to the full Cu-valence change at the intersite CT transition of the analog LaCu<sub>3</sub>Fe<sub>4</sub>O<sub>12</sub> (LaCu<sup>2+</sup><sub>3</sub>Fe<sup>3.75+</sup><sub>4</sub>O<sub>12</sub> ↔ LaCu<sup>3+</sup><sub>3</sub>Fe<sup>3+</sup><sub>4</sub>O<sub>12</sub>) at T<sub>CT</sub> = 393 K, which is accompanied by a metal-insulator transition [20]. As the magnetic susceptibility of LaCu<sub>3</sub>Cr<sub>4</sub>O<sub>12</sub> below T<sub>CT</sub> is very small and temperature independent, the low temperature phase of LaCu<sub>3</sub>Cr<sub>4</sub>O<sub>12</sub> was expected to be a Pauli paramagnetic metal like CaCu<sub>3</sub>Cr<sub>4</sub>O<sub>12</sub> and ACu<sub>3</sub>V<sub>4</sub>O<sub>12</sub> (A = Na, Ca, and Y) which also have mixed-valent Cu, Cr, and V ions [21, 22]. However, the present magnetic structure analysis from neutron powder diffraction (NPD) reveals an unexpected G-type magnetic ordering in the low-temperature conducting phase of LaCu<sub>3</sub>Cr<sub>4</sub>O<sub>12</sub>.

A polycrystalline sample of LaCu<sub>3</sub>Cr<sub>4</sub>O<sub>12</sub> was prepared under a high-pressure (9 GPa) and high-temperature (900 °C) condition using a cubic-anvil-type high-pressure apparatus as reported previously [19]. Electrical resistivity was measured on a dense pellet using the standard 4-probe technique and magnetization was measured using a SQUID magnetometer. Both data show an anomaly at T<sub>CT</sub> = 220 K (Figs. 1(b) and (c)) but metallic conduction both above and below T<sub>CT</sub> is seen in the resistivity plot. The measured resistivity (5 mΩ cm at room temperature) is much lower than those of polycrystalline ACrO<sub>3</sub> (A = Ca, Sr) in the same temperature range [8] and is comparable to that of the Pauli paramagnetic metal CaCu<sub>3</sub>Cr<sub>4</sub>O<sub>12</sub> (1 mΩ cm) [21]. Although a grain boundary effect in the polycrystalline sample causes the resistivity to increase slightly below ~70 K, the small residual resistivity of 10 mΩ cm shows that the intrinsic ground state is metallic. The small almost temperature independent magnetic susceptibility below T<sub>CT</sub> excludes the possibilities of a ferro- or ferri-magnetic ground state, or of a further magnetic or metal-insulator transition below T<sub>CT</sub>.

Time-of-flight NPD experiments on a 70 mg polycrystalline sample of LaCu<sub>3</sub>Cr<sub>4</sub>O<sub>12</sub> were performed at the WISH and GEM beamlines (ISIS Rutherford Appleton Laboratory, UK). Diffraction data were collected at 5, 200, 250 and 300 K up to a d-spacing of ~10 Å. Rietveld refinements of the crystal and magnetic structures were carried out using the FULLPROF program [23]. The NPD pattern at 300 K was reproduced well with the Im-3 structure model with cubic cell parameter a = 7.3198(2) Å. The refinement results (see Supplemental Material [24]), representing an A-site-ordered perovskite structure with Cu at the square-planar A' sites and Cr at the octahedral B sites, are consistent with the results of our previous synchrotron XRD study [19].

Although the ground state had been expected to be Pauli paramagnetic, magnetic reflections breaking the body-centered symmetry of the crystal structure, such as 1 1 1, 1 1 3, and 1 3 3, were clearly seen in the diffraction pattern obtained at 5 K (Fig. 2), demonstrating the existence of a long-range magnetic order with propagation vector (1 1 1). These peaks are fitted well with a collinear G-type AFM arrangement of the B-site Cr spins as shown and the refined magnetic moment at 5 K is 1.60(1) μ<sub>B</sub>. No other magnetic peaks were observed. AFM orders of the

$A'$ -site Cu moments are excluded as these would result in further magnetic reflections such as 0 0 1, 2 0 1, and 2 2 1. No magnetic intensities arising from (0 0 0) ferromagnetic Cu or Cr orders were observed, these orders are also excluded by the absence of ferromagnetic behavior in the magnetization measurements [19]. The fitting results for the 5 K diffraction data are shown in Fig. 2, with the spin structure inset (although absolute spin directions in a cubic material are not determined in a NPD experiment). The refined structural parameters at 5 K are summarized in Table I and selected bond distances and bond angles are given in Supplemental Material [24]. The accurate metal-oxygen distances obtained from NPD enable the formal charges of the Cu and Cr ions to be estimated using the bond valence sum method, and the results confirm a charge-transferred ground state with formal charge distribution  $\text{LaCu}^{2.5+}_3\text{Cr}^{3.4+}_4\text{O}_{12}$  ( $\gamma=0.5$ ), demonstrating the presence of a substantial Cu/Cr band overlap. The details of the calculations for 300, 250, 200 and 5 K structures are presented in Supplemental Material [24]. The G-AFM order of the Cr spins are also observed in the NPD patterns at 200 K just below  $T_{\text{TC}}$ , and the refined magnetic moment of the  $B$ -site Cr spins is  $1.45(3) \mu_{\text{B}}$ . The observed moment is comparable to that at 5 K, indicating that the intrinsic magnetic correlation temperature is much higher than  $T_{\text{CT}}$ , as seen in the temperature dependence of magnetic moment in the charge transferred  $\text{LaCu}_3\text{Fe}_4\text{O}_{12}$  [25, 26]. Thus, the simultaneous magnetic transition is induced by the CT transition.

It is now evident that the Cr ions at the  $B$  sites have substantial magnetic moments at temperatures below  $T_{\text{CT}} = 220$  K. The refined moment of  $1.6 \mu_{\text{B}}$  at 5 K is reduced from the ideal value of  $2.7 \mu_{\text{B}}$  for the weighted average of  $\text{Cr}^{3+}(S=3/2)$  and  $\text{Cr}^{4+}(S=1)$  ions, reflecting the strong hybridization between oxygen  $2p$  and Cr  $3d$  orbitals. This 40% moment reduction is identical to that in metallic  $\text{CaCrO}_3$  where a  $1.2 \mu_{\text{B}}$  moment was reported for  $\text{Cr}^{4+}$  [7]. The formal  $\text{Cu}^{2.5+}$  state would allow a small moment, but as each Cu site is connected equally to four up and four down Cr spins then possible order of Cu spins is highly frustrated and no ordered moment is observed at 5 K.

The origin of the itinerant  $3d$  electrons in  $\text{LaCu}_3\text{Cr}_4\text{O}_{12}$  is different from that in the conducting antiferromagnets  $\text{CaCrO}_3$  and  $\text{SrCrO}_3$ , where orbital ordering of the  $\text{Cr}^{4+} t_{2g}$  states leads to C-type antiferromagnetism [7–9,17]. Degeneracy of the Cr  $t_{2g}$  orbitals is partly lifted through distortion of the  $\text{CrO}_6$  octahedra, yielding both localized and itinerant electrons. However, in  $\text{LaCu}_3\text{Cr}_4\text{O}_{12}$ , there is no change in structural symmetry below  $T_{\text{CT}}$  and the  $\text{CrO}_6$  octahedra are almost undistorted, as they have  $-3$  symmetry with six equal Cr–O distances and O–Cr–O bond angles very close to  $90^\circ$  (with only a  $0.1^\circ$  deviation at 5 K [24]). The Cr  $t_{2g}$  levels in such an isotropic coordination are expected to be degenerate so it is surprising that mixed itinerant electrons and local moments arise here.

The electronic structure of  $\text{LaCu}_3\text{Cr}_4\text{O}_{12}$  has been calculated by the full-potential linearized augmented plane-wave (LAPW) method within the generalized gradient approximation with the WIEN2k code [27]. The experimental lattice constant and the atomic coordinates from the 5 K NPD refinement were used for the calculation. LAPW sphere radii were 2.0, 1.9, 1.9, and 1.6 a.u. for La, Cu, Cr, and O, respectively. Self-consistency was carried out on 45  $k$ -point meshes in the irreducible Brillouin zone. The *ab initio* calculations reveal key features of the electronic structure. A spin polarized model with nonmagnetic Cu and G-type AFM Cr spins was found to give a lower total energy than a non-polarized one with both nonmagnetic Cu and Cr ions, and ferrimagnetic case with antiferromagnetically coupled FM sublattices of Cu and Cr spins by 2.07 and 0.16 eV/f.u., respectively. Calculation of a ferromagnetic model converged to a ferrimagnetic one. When electron correlations

are taken into account in the calculations, essentially the same results with different stabilization energies are obtained, as listed in Supplemental Material. The calculated band structure of the up spin and the corresponding density of states (DOSs) of the lowest energy model by the standard calculation without  $U_{\text{eff}}$  are shown in Fig. 3 (see also in Supplemental Material). The calculated magnetic moments inside the muffin tin spheres are 0.00 and  $\pm 1.97 \mu_B$  for Cu and Cr ions respectively, in good agreement with the refined values in the magnetic structure analysis. Each Cr ion is highly spin polarized, and the bands just below the Fermi level ( $E_F$ ) mainly consist of the Cr-3*d* and O-2*p* orbitals. The main feature of the electronic structure near  $E_F$  is that the Cu-3*d* orbitals just above  $E_F$  are strongly hybridized with Cr-3*d* and O-2*p* orbitals, and the bottom of the bands touches  $E_F$  at the R point. The top of the valence bands, which mainly consist of Cr-3*d* and O-2*p* orbitals, also touches  $E_F$  at the  $\Gamma$  point, giving a gapless band structure, suggesting that this itinerant system is in the vicinity of localization. The heavy tilting of the CrO<sub>6</sub> octahedra with a Cr–O–Cr bond angle of 139.9(1)<sup>°</sup> narrows the Cr-3*d* bands, and the hybridization of Cr-3*d* and Cu-3*d* bands stabilizes the delicate electronic structure near an itinerant-localized crossover. The spin polarization of the mixed valent Cr ions is thus induced by the involvement of the Cu-3*d* orbital in the orbital hybridization. Such a nearly localized nature of the Cr moment is also observed in the high-temperature phase above  $T_{\text{CT}}$ , where the magnetic susceptibility is rather large and temperature-dependent.

Metallicity in magnetically ordered oxides usually requires ferromagnetically coupled spin networks to enhance electron transfer. A G-type AFM structure where all NN spin pairs are coupled antiferromagnetically has not been reported previously in any metallic perovskites. In LaCu<sub>3</sub>Cr<sub>4</sub>O<sub>12</sub> the G-type AFM structure is stabilized by NN AFM superexchange interactions between essentially localized Cr spins. Importantly, this results in ferromagnetically coupled NNN Cr spins bridged by Cr( $\uparrow$ )–O–Cu–O–Cr( $\uparrow$ ) pathways through 180<sup>°</sup> O–Cu–O bonds, and the resulting strong orbital hybridization and Cr/Cu charge transfer facilitate spin-polarized conduction in the {1 1 1} layers of FM spins. In other words, the ferromagnetic {1 1 1} layers of the G-type antiferromagnetic Cr-spin sublattice allow the spin-polarized electron transfer through the strongly hybridized Cu orbitals. Simple *ABO*<sub>3</sub> perovskites lack such strongly hybridized NNN connections so G-type antiferromagnets such as LaFeO<sub>3</sub>, LaCrO<sub>3</sub>, CaMnO<sub>3</sub> etc. are insulating. Coexistence of metallicity and magnetic order may also result from RKKY interactions or a Fermi surface instability. In the present LaCu<sub>3</sub>Cr<sub>4</sub>O<sub>12</sub>, however, the DOS at the  $E_F$  in the nearly gapped electronic structure in the vicinity of localized electron system is too low to produce such a strong magnetic correlation. Thus, the superexchange scenario is the most appropriate to explain the magnetism in LaCu<sub>3</sub>Cr<sub>4</sub>O<sub>12</sub>.

In conclusion, neutron diffraction demonstrates that the low-temperature phase of the metallic *A*-site-ordered perovskite LaCu<sub>3</sub>Cr<sub>4</sub>O<sub>12</sub> below the 220 K charge transfer transition has G-type long range antiferromagnetic order at the octahedral Cr sites and no ordered moments at the square-planar Cu sites. This G-type ordering of *B*-site transition metal ion spins in a metallic perovskite system is unprecedented. Both Cu and Cr ions with mixed valence states contribute to the metallic conduction. Narrowing of Cr-O-Cr bands due to heavy tilting of the CrO<sub>6</sub> octahedra and strong hybridization of Cu-3*d*, Cr-3*d* and O-2*p* orbitals result in an unusual electronic structure in the vicinity of a localized-electron regime. The G-type antiferromagnetic ordering of the nearly localized Cr spins is stabilized by a conventional nearest-neighbor antiferromagnetic superexchange interaction. The ferromagnetic {1 1 1} layers of the G-type antiferromagnetic Cr-spin sublattice allow the spin-polarized electron transfer through the strongly hybridized Cr-O-Cu-O-Cr orbitals. Hence, even the ‘most antiferromagnetic’ G-type spin ordering

configuration on a primitive cubic lattice where all nearest neighbor pairs are antiparallel can still support metallicity in oxide perovskites.

We thank Y. Hosaka and F. D. Romero in Kyoto University (Japan) and H. Johnston and G. McNally in the University of Edinburgh (UK) for the help during the NPD measurements. This work was performed under the Strategic Japanese-UK Cooperative Program by Japan Science and Technology Agency (JST), Engineering and Physical Sciences Research Council (EPSRC), and Core-to-Core Program (JSPS and EPSRC). This work was partly supported by Grants-in-Aid for Scientific Research (Nos. 19GS0207, 22740227, 24540346, 16H00888, and 16H02266) and by a grant for the Integrated Research Consortium on Chemical Sciences from the Ministry of Education, Culture, Sports, Science and Technology (MEXT) of Japan. The work was also supported by Japan Science and Technology Agency, CREST. Support was also provided by EPSRC, STFC and the Royal Society, UK.

\*saito@scl.kyoto-u.ac.jp

- [1] J. M. Longo, P. M. Raccah and J. B. Goodenough, *J. Appl. Phys.* **39**, 1327 (1968).
- [2] C. Zener, *Phys. Rev.* **82**, 403 (1951).
- [3] M. A. Korotin, V. I. Anisimov, D. I. Khomskii, and G. A. Sawatzky, *Phys. Rev. Lett.* **80**, 4305 (1998).
- [4] K.-I. Kobayashi, T. Kimura, H. Sawada, K. Terakura, and Y. Tokura, *Nature* **395**, 677 (1998).
- [5] D. N. Argyriou, J. F. Mitchell, P. G. Radaelli, H. N. Bordallo, D. E. Cox, M. Medarde, and J. D. Jorgensen, *Phys. Rev. B* **59**, 8695 (1999).
- [6] Y. Yoshida, S. I. Ikeda, H. Matsuhata, N. Shirakawa, C. H. Lee, and S. Katano, *Phys. Rev. B* **72**, 054412 (2005).
- [7] A. C. Komarek, S. V. Streltsov, M. Isobe, T. Möller, M. Hoelzel, A. Senyshyn, D. Trots, M. T. Fernández-Díaz, T. Hansen, H. Gotou, T. Yagi, Y. Ueda, V. I. Anisimov, M. Grüninger, D. I. Khomskii, and M. Braden, *Phys. Rev. Lett.* **101**, 167204 (2008).
- [8] A. C. Komarek, T. Möller, M. Isobe, Y. Drees, H. Ulbrich, M. Azuma, M. T. Fernández-Díaz, A. Senyshyn, M. Hoelzel, G. André, Y. Ueda, M. Grüninger, and M. Braden, *Phys. Rev. B* **84**, 125114 (2011).
- [9] L. Ortega-San-Martin, A. J. Williams, J. Rodgers, J. P. Attfield, G. Heymann, and H. Huppertz, *Phys. Rev. Lett.* **99**, 255701 (2007).
- [10] J. B. Goodenough, J. M. Longo, and J. A. Kafalas, *Mat. Res. Bull.*, **3**, 471 (1968).
- [11] J. F. Weiher, B. L. Chamberland, and J. L. Gillson, *J. Solid State Chem.* **3**, 529 (1971).
- [12] J. S. Zhou, C. Q. Jin, Y. W. Long, L. X. Yang, and J. B. Goodenough, *Phys. Rev. Lett.* **96**, 046408 (2006).
- [13] Y. W. Long, L. X. Yang, Y. X. Lv, Q. Q. Liu, C. Q. Jin, J. S. Zhou and J. B. Goodenough, *J. Phys.: Condens. Matter* **23**, 355601 (2011).
- [14] B. L. Chamberland, *Solid State Commun.* **5**, 663 (1967).
- [15] A. J. Williams, A. Gillies, J. P. Attfield, G. Heymann, H. Huppertz, M. J. Martínez-Lope, and J. A. Alonso, *Phys. Rev. B* **73**, 104409 (2006).
- [16] P. A. Bhohe, A. Chainani, M. Taguchi, R. Eguchi, M. Matsunami, T. Ohtsuki, K. Ishizaka, M. Okawa, M. Oura, Y. Senba, H. Ohashi, M. Isobe, Y. Ueda, and S. Shin, *Phys. Rev. B* **83**, 165132 (2011).
- [17] K.-W. Lee and W. E. Pickett, *Phys. Rev. B* **80**, 125133 (2009).
- [18] Y. Shimakawa, *Inorg. Chem.* **47**, 8562 (2008).

- [19] S. Zhang, T. Saito, M. Mizumaki, and Y. Shimakawa, *Chem. Eur. J.* **20**, 9510 (2014).
- [20] Y. W. Long, N. Hayashi, T. Saito, M. Azuma, S. Muranaka, and Y. Shimakawa, *Nature* **458**, 60 (2009).
- [21] M. A. Subramanian, W. J. Marshall, T. G. Calvarese, and A. W. Sleight, *J. Phys. Chem. Solids* **64**, 1569 (2003).
- [22] H. Shiraki, T. Saito, M. Azuma, and Y. Shimakawa, *J. Phys. Soc. Jpn.* **77**, 064705 (2008)
- [23] FULLPROF: D. B. Wiles and R. A. Young, *J. Applied Cryst.* **14**, 149 (1981).
- [24] See Supplemental Material at [URL will be inserted by publisher] for more details on the Rietveld refinement of the NPD data, bond valence sum calculations, and *ab initio* electronic structure calculation.
- [25] W. T. Chen, Y. W. Long, T. Saito, J. P. Attfield, and Y. Shimakawa, *J. Mater. Chem.* **20**, 7282 (2010).
- [26] Y. Shimakawa, *J. Phys. D: Appl. Phys.* **48**, 504006 (2015).
- [27] P. Blaha, K. Schwarz, G. Madsen, D. Kvasnicka and J. Luitz, WIEN2k, An Augmented Plane Wave + Local Orbitals Program for Calculating Crystal Properties (Karlheinz Schwarz, Techn. Universität Wien, Austria), 2001. ISBN 3-9501031-1-2

## TABLES

Table I. Results of the Rietveld refinement of the neutron powder diffraction data for  $\text{LaCu}_3\text{Cr}_4\text{O}_{12}$  at 5 K. The Wyckoff positions in space group  $Im\bar{3}$ , coordinates, isotropic atomic displacement parameter  $B_{\text{iso}}$ , site occupancy, size of the magnetic moment  $M_{8c}$  at the  $8c$  Cr site, and lattice parameter are listed together with the reliability factors. Numbers in parentheses are standard deviations of the last significant digit.

Atom	Wyckoff pos.	$x$	$y$	$z$	$B_{\text{iso}} (\text{\AA}^2)$	Occ.
La	$2a$	0	0	0	0.81(8)	1
Cu	$6b$	0	$\frac{1}{2}$	$\frac{1}{2}$	0.54(5)	1
Cr	$8c$	$\frac{1}{4}$	$\frac{1}{4}$	$\frac{1}{4}$	0.30(7)	1
O	$24g$	0	0.1772(1)	0.3068(1)	0.68(5)	1
$M_{8c} = 1.60(1) \mu_{\text{B}}/\text{Cr}$ , $a = 7.31120(3) \text{\AA}$						
$R_{\text{wp}} = 1.83\%$ , $R_{\text{B}}(\text{nuclear}) = 3.13\%$ , $R_{\text{B}}(\text{magnetic}) = 6.01\%$						

## FIGURE CAPTIONS

FIG. 1. (Color online) (a) Crystal structure of the  $A$ -site-ordered perovskite  $\text{LaCu}_3\text{Cr}_4\text{O}_{12}$ . Temperature dependence of (b) resistivity and (c) magnetic susceptibility of  $\text{LaCu}_3\text{Cr}_4\text{O}_{12}$ . Temperature dependence of inverse magnetic susceptibility is also plotted on the right. (reproduced from ref. 19)

FIG. 2. (Color online) Rietveld plot of the neutron powder diffraction pattern at 5 K. The observed (+) and calculated (red line) patterns are shown, as is the difference between them (blue line). The ticks indicate the allowed Bragg reflections for nuclear (top) and magnetic (middle) phases of  $\text{LaCu}_3\text{Cr}_4\text{O}_{12}$  and the vanadium container (bottom). Magnetic structure of  $\text{LaCu}_3\text{Cr}_4\text{O}_{12}$  is shown in the inset.

FIG. 3. (Color online) Calculated DOSs for up-spin and down-spin electrons for G-type AFM  $\text{LaCu}_3\text{Cr}_4\text{O}_{12}$ . Total DOS (shaded) and partial DOS of Cu (blue), up-spin Cr (red), and O (black) are shown.  $E_F$  is the Fermi energy. The up spin band structure is shown on the right.

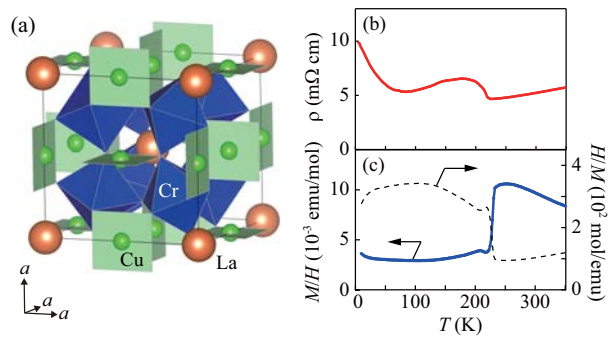


Fig. 1

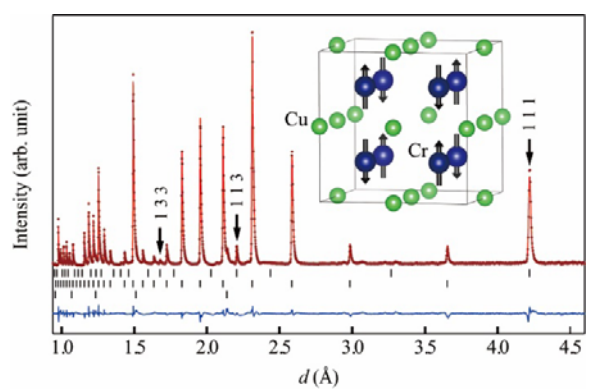


Fig. 2

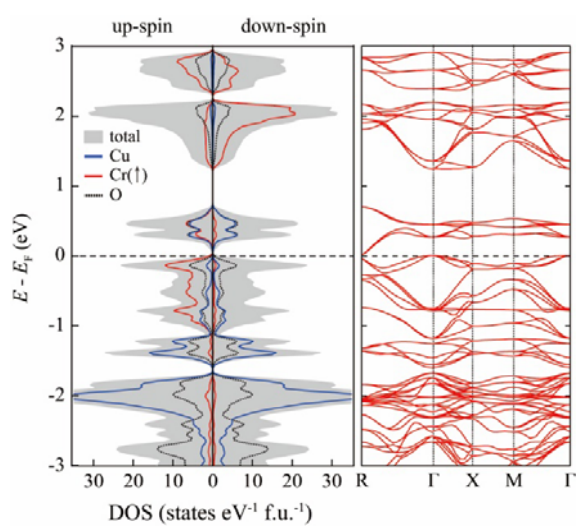


Fig. 3